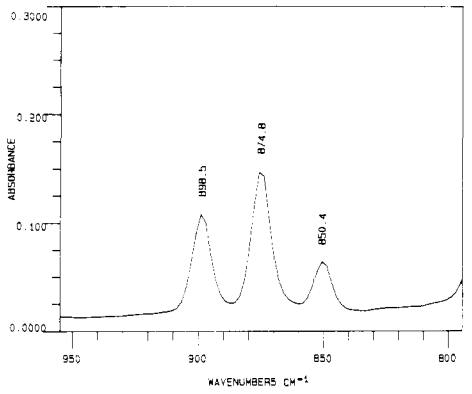

Figure 5. Infrared difference spectrum in the O–O stretching region for a mixture of peroxo complexes of a $MnPEt_3Br_2$ film exposed to a mixture of $^{16}O_2$, $^{16}O^{18}O$, and $^{18}O_2$ at −30 °C (see text).

= 1:1) over a 2-h period at −30 °C. The O–O stretching region of the infrared spectra recorded following each of these operations is shown in Figure 4. Figure 4a illustrates the development of the $^{18}O_2$ peroxo species, Figure 4b its loss upon evacuation, Figure 4c its reappearance, and Figure 4d the formation of a $^{16}O_2$ peroxo species. The $^{18}O_2$ band declined in intensity somewhat during the development of the $^{16}O_2$ band. The two isotopic diatomic oxygen species are thus freely exchanging with the manganese complex. It has been suggested to us that the loss of intensity of the $^{18}O_2$ peroxo band during the development of the $^{16}O_2$ band could be due to decomposition of the peroxo species to a phosphine oxide product rather than to reversible interaction with dioxygen.[16] To evaluate this possibility, we sublimed 100 mg of $MnBr_2$ onto a cold finger of surface area 61.4 cm^2 in a specially designed Dewar, degassed at 10^{-6} Torr, exposed the film to the vapor pressure of triethyl phosphine, evacuated at 10^{-6} Torr for 4 h, and exposed the complex film to 25 Torr of $^{16}O_2$ for 150 min and then 760 Torr for 60 min at −30 °C to produce a deep red color but no measurable pressure drop. Then the oxygenated complex was cooled to −100 °C while the excess O_2 was evacuated (to 10^{-6} Torr); the red color remained. Finally the sample was allowed to warm to ambient temperature, with all desorbed gas (3.5 Torr) being trapped. Mass spectral analysis showed the desorbed gas to be primarily $^{16}O_2$ with a small amount of CO as an impurity from the vacuum system. We believe that this experiment demonstrates conclusively that a reversible interaction of the complex with dioxygen at −30 °C is occurring.

The weak broad feature at ca. 870 cm^{-1} in Figure 4 could be due to an ^{16}O–^{18}O peroxo species, which would be indicative of partial dissociation of dioxygen on manganese. Mass spectrometric sampling of the gases in the cell at −30 °C revealed no m/e = 34 peak indicative of $^{16}O^{18}O$. However, upon warming the sample to ambient temperature during evacuation, an m/e = 34 peak in the mass spectrum appeared and actually eventually exceeded the intensities of the m/e = 36 and m/e = 32 peaks. We found that the cracking pattern for triethylphosphine also contains a large m/e = 34 peak (presumably due to PH_3^+) with our mass spectrometer (Molytek SM 1000M) under similar conditions. Thus the weak infrared band at 870 cm^{-1} may be due to a ligand decomposition product rather than to a $^{16}O^{18}O$ peroxo species. To test these hypotheses, an authentic sample of $^{16}O^{18}O$ was prepared by electrical discharge through a mixture of 11.2 Torr of $^{16}O_2$ and 9.7 Torr of $^{18}O_2$ to produce a mixture containing (mass spectrometric analyses) a ratio of 3.0 parts $^{16}O_2$, 3.45 parts $^{16}O^{18}O$, and 1.0 part $^{18}O_2$. Any ozone produced was removed by condensation on molecular sieves at 77 K. Then 16.5 Torr of this mixture of dioxygen species was interacted with an $MnPEt_3Br_2$ film at −30 °C for 4.5 h, and the infrared spectrum shown in Figure 5 was recorded. It is evident that the authentic $^{16}O^{18}O$ species exhibits its infrared band at 875 cm^{-1}, not at 870 cm^{-1} as for the species represented in Figure 4. Furthermore, the $^{16}O^{18}O$ band in Figure 5 has the same width profile as do the $^{16}O_2$ and $^{18}O_2$ peroxo species bands but unlike the broad profile of the 870-cm^{-1} band in Figure 4. Therefore, we conclude that the 870-cm^{-1} band in Figure 4 refers to a small amount of ligand decomposition product rather than to a $^{16}O^{18}O$ species.

Conclusions

In summary, this work has demonstrated a reversible interaction of dioxygen and $MnPEt_3Br_2$ to form a side-on peroxo species (red) at low temperature (−30 °C). As reported previously,[4] at higher temperature (ambient and above) the interaction of dioxygen, which may or may not be reversible, with the manganese complex film produces a superoxo species (blue), which decomposes irreversibly to an inactive phosphine oxide complex.

Acknowledgment. We thank the Office of Naval Research for support of this work.

(16) We acknowledge a reviewer for this suggestion.

Chemielectron Spectroscopy: Study of the Ce + O_2 Reaction

M. C. R. Cockett, J. M. Dyke,* A. M. Ellis, M. Fehér, and A. Morris

Contribution from the Department of Chemistry, The University, Southampton, SO9 5NH U.K.
Received February 17, 1988

Abstract: The chemielectron and mass-resolved ion spectra produced from the Ce + O_2 reaction have been recorded. The mass spectrum together with approximate thermochemical and kinetic calculations have been used to show that the major chemiionization channel for this reaction under thermal conditions is the associative ionization process, Ce + O_2 → CeO_2^+ + e^-. The electron spectrum has been interpreted in terms of this process via a classical turning-point mechanism. CeO_2^+ and CeO^+ are observed as reaction products in the mass-resolved ion spectrum. CeO_2^+ arises almost completely from the above associative ionization reaction, whereas CeO^+ is shown to arise from more than one reaction in the Ce + O_2 reaction scheme.

The importance of chemiionization reactions in flames,[1,2] upper atmosphere chemistry,[3] and in shock waves and detonations[4,5] has led to a large number of these reactions being identified in recent years. However, for most of these reactions virtually nothing is known about the mechanism of the ionization process. Many chemiionization reactions produce free electrons whose energy distribution can be measured by electron spectroscopy. These

* To whom correspondence should be addressed.

(1) Calcote, H. G. *Combust. Flame* **1981**, *42*, 215.
(2) Fontijn, A. *Prog. React. Kinet.* **1971**, *6*, 75.
(3) Brown, T. L. *Chem. Rev.* **1973**, *73*, 645.
(4) Matsuda, S.; Gutman, D. *J. Chem. Phys.* **1971**, *54*, 453.

0002-7863/89/1511-5994$01.50/0

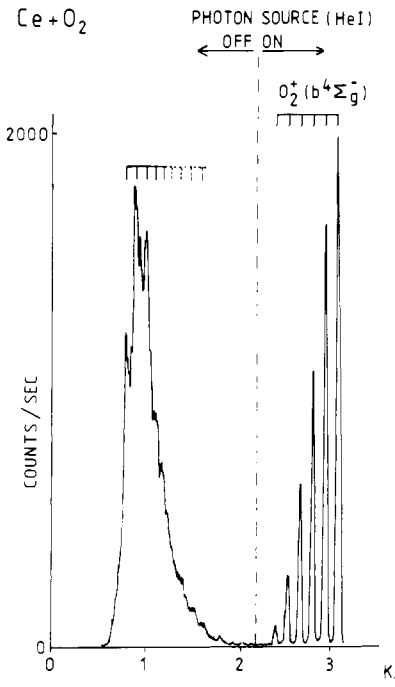

Figure 1. Chemielectron spectrum obtained for the Ce + O_2 reaction: ordinate, count s^{-1}; abscissa, electron kinetic energy (electronvolts).

"chemielectron spectroscopic" studies are valuable because it is possible to use the measured electron energy distribution to obtain some information on the mechanism of the chemiionization process.[6] Chemielectron spectroscopy has recently been used to study several gas-phase chemiionization reactions of metals and metal oxides with suitable oxidants[7-9] and, as part of these chemielectron spectroscopic studies, the gas-phase chemiionization reaction between atomic cerium and molecular oxygen is investigated here. This reaction has been studied previously by mass spectrometry using both accelerated cerium beams[10] and thermal reactants.[11] At thermal collision energies two different chemiionization channels were observed leading to the formation of CeO^+ and CeO_2^+, the relative cross sections for these channels being approximately 1:30.[12]

The aim of this work was to record the chemielectron spectrum from the Ce + O_2 reaction and identify the cationic products under the same experimental conditions using mass spectrometry. The combined results are then used to develop a more detailed picture of the reaction mechanism using schematic potential energy diagrams.

Experimental Section

Cerium was produced in the vapor phase by evaporating solid cerium (Cerac Inc, 99.9%) from an inductively heated molybdenum furnace attached to a single detector photoelectron spectrometer. This apparatus has been described in detail elsewhere.[13,14] Oxygen was added at right angles to the cerium effusive beam in the ionization chamber of the spectrometer, and chemielectron spectra arising from the reaction were recorded with the hemispherical analyzer, detector, and associated electronics of the photoelectron spectrometer. In these experiments, the photon source of the spectrometer was usually blocked with a shutter, although to calibrate the electron energy scale of the electron spectra obtained, part of the spectral range was recorded with a He I (21.22 eV) photon source with the shutter removed. This enabled calibrated chemielectron spectra with high signal-to-noise ratios to be recorded. Calibration of the Ce + O_2 chemielectron spectra was achieved using the HeI photoelectron spectrum of oxygen.

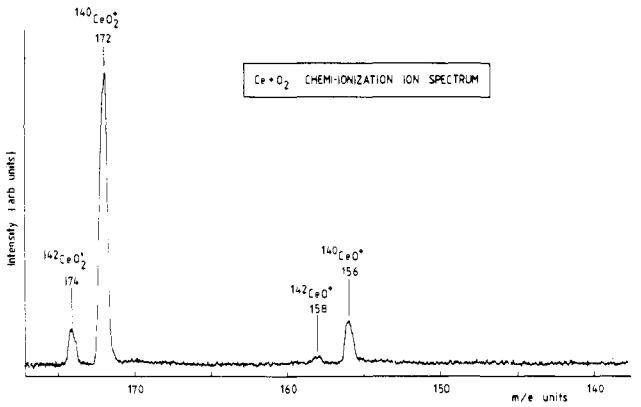

Figure 2. Mass spectrum obtained under conditions identical with those used to obtain Figure 1.

As well as these chemielectron experiments, the cationic products of the Ce + O_2 chemiionization reaction, produced using the same conditions, were identified with a quadrupole mass spectrometer (SX 200F, VG Quadrupoles) in which the electron impact ionization source of the mass spectrometer had been switched off so that only ions produced by chemiionization were detected. The reactants, Ce and O_2, were mixed inside a partially enclosed reaction cell. Positively charged chemiions were extracted from the reaction cell and were focused into the mass spectrometer with a three-element aperture–lens system.

Results and Discussion

The chemielectron spectrum obtained from the reaction of cerium with oxygen at a furnace temperature of 1650 ± 50 K is shown in Figure 1. In this spectrum, one band was observed with a maximum at 0.90 ± 0.04 eV electron kinetic energy. It is highly asymmetric, has an onset of 0.61 ± 0.10 eV, and has a tail extending nearly 1 eV beyond the maximum. Regular vibrational structure was also observed in this band, and measurement of this structure gave an average separation of 790 ± 30 cm^{-1}. This band was observed for the Ce + O_2 reaction when cerium was evaporated from either a molybdenum or a tungsten furnace.

The mass spectrum recorded under conditions identical with those used to obtain the chemielectron spectrum in Figure 1 is shown in Figure 2. This can be readily assigned to the CeO_2^+ and CeO^+ ions as the ^{140}Ce:^{142}Ce natural abundance ratio is 7.97:1 and the CeO^+ and CeO_2^+ signals both showed two components that were, within experimental error, in this intensity ratio (see Figure 2). The CeO_2^+:CeO^+ intensity ratio was observed to be (7.5 ± 0.8):1, for oxygen pressures in the region 1×10^{-5}–8×10^{-4} Torr, in poor agreement with the relative cross sections for production of CeO_2^+ and CeO^+ of 30:1 measured previously by mass spectrometry.[11,12]

Four primary chemiionization channels are possible in the Ce + O_2 reaction. These are

$$Ce + O_2 \rightarrow CeO_2^+ + e^- \quad (1)$$

$$Ce + O_2 \rightarrow CeO^+ + O^- \quad (2)$$

$$Ce + O_2 \rightarrow CeO^+ + O + e^- \quad (3)$$

$$Ce + O_2 \rightarrow Ce^+ + O_2^- \quad (4)$$

The thermodynamic threshold energies for these processes can be calculated as 0.49 ± 0.42, 0.38 ± 0.26, 1.84 ± 0.26, and 5.099 ± 0.009 eV, respectively, with use of literature values for the dissociation energy of CeO,[15] the atomization energy of CeO_2,[16]

(5) Cavenor, M. C.; Monday, G.; Ubbelhode, A. R. *Combust. Flame* **1972**, *18*, 99.
(6) Berry, R. S. *Adv. Mass Spectrom.* **1974**, *6*, 1.
(7) Dyke, J. M.; Fehēr, M.; Gravenor, B. W. J.; Morris, A. *J. Phys. Chem.* **1987**, *91*, 4476.
(8) Dyke, J. M. *J. Chem. Soc., Faraday Trans. 2* **1987**, *83*, 69.
(9) Dyke, J. M.; Ellis, A. M.; Fehēr, M.; Morris, A. *Chem. Phys. Lett.* **1988**, *145*, 159.
(10) Young, C. E.; Cohen, R. B.; Dehmer, P. M.; Pobo, L. G.; Wexler, S. *J. Chem. Phys.* **1976**, *65*, 2562.
(11) Lo, H. H. Unpublished data quoted in ref 12.
(12) Fite, W. L.; Patterson, T. A.; Siegel, M. W. US Air Force Report AFGL-TR-77-0030, 1976.
(13) Dyke, J. M.; Jonathan, N.; Morris, A. *Int. Rev. Phys. Chem.* **1982**, *2*, 3.
(14) Bulgin, D.; Dyke, J. M.; Goodfellow, F.; Jonathan, N.; Lee, E.; Morris, A. *J. Electron. Spectrosc. Relat. Phenom.* **1977**, *12*, 67.
(15) Coppens, P.; Smoes, S.; Drowart, J. *Trans. Faraday Soc.* **1967**, *63*, 2140.

the first ionization energy of CeO[17] and CeO_2,[18] the dissociation energy of O_2,[19] the electron affinity of O,[20] the ionization energy of cerium,[21] and the electron affinity of O_2.[22] On the basis of these reaction thresholds, reactions 3 and 4 are the most endothermic, and the main channels for production of CeO^+ and CeO_2^+ under thermal conditions might be expected to be reactions 1 and 2. Of these two reactions, as reaction 1 is the only one that produces electrons, and as CeO_2^+ is the most intense ion signal seen in Figure 2, the most obvious explanation for the structured electron band seen in Figure 1 is that it is associated with electrons produced from reaction 1.

According to the thermodynamic thresholds quoted above, reaction 1 is endothermic. If the calculated threshold of 0.49 ± 0.42 eV for this reaction is assumed to be correct, then to produce chemielectrons with a kinetic energy of 0.90 eV, the maximum of the chemielectron band in Figure 1, the reactants would need an excess energy of approximately 1.4 eV. However, there appears to be no way in which this excess energy, whether in the form of electronic excitation energy of cerium or relative reactant collision energies, could be produced at the furnace temperatures used. Hence, it appears that the thermodynamic data used in calculating the threshold for reaction 1 are unreliable. In the calculation of this threshold the dissociation energy ($D_0°$) of oxygen, the atomization energy of CeO_2 and the first ionization energy of CeO_2 are needed. As $D_0°$ for O_2 is well established at 5.115 ± 0.002 eV,[19] the atomization energy of CeO_2 (14.92 ± 0.22 eV[16]) and the first ionization energy of CeO_2 (10.3 ± 0.2 eV[18]) are both possible sources of this error. The atomization energy of CeO_2 of Kordis and Gingerich[16] seems the most reliable available. However, the first ionization energy of CeO_2 has been determined in a number of independent studies by electron impact mass spectrometry as 10.3 ± 0.2,[18] 9.8 ± 0.5,[23] and 9.5 ± 0.5 eV,[24] and it is difficult to determine which is the most reliable result. The value of 10.3 ± 0.2 eV[18] was initially selected in this present work because it has the lowest quoted error. However, the lower values of 9.8 ± 0.5[23] and 9.5 ± 0.5 eV[24]seem more reasonable in the light of the experimental chemielectron spectrum. This uncertainty would obviously be removed if the photoelectron spectrum of gaseous CeO_2 was available. Nevertheless, if the first ionization energy of CeO_2 is taken as 9.5 ± 0.5 eV,[24] the threshold for reaction 1 is calculated as −0.31 ± 0.72 eV, a value more in line with the band maximum of 0.90 eV measured in Figure 1, particularly when the error limits of the derived value are taken into account.

One other problem that occurs in the present study is the discrepancy that exists between the experimental CeO_2^+:CeO^+ ion intensity ratio of (7.5 ± 0.8):1 shown in Figure 2 and that quoted in ref 12 of 30:1 as determined in a Ce + O_2 crossed-beam study. The first possible source of this difference to be checked was that mass-dependent changes in ion transmission occurred as a function of the extraction voltage into the quadrupole analyzer. To investigate this possibility, the CeO_2^+:CeO^+ ion intensity ratio was recorded as a function of ion kinetic energy into the quadrupole rods over the energy range 7–60 eV at constant reagent partial pressure. The measured CeO_2^+:CeO^+ intensity ratio was, within experimental error, unchanged, eliminating this source as the origin of the observed difference in ion intensity ratios.

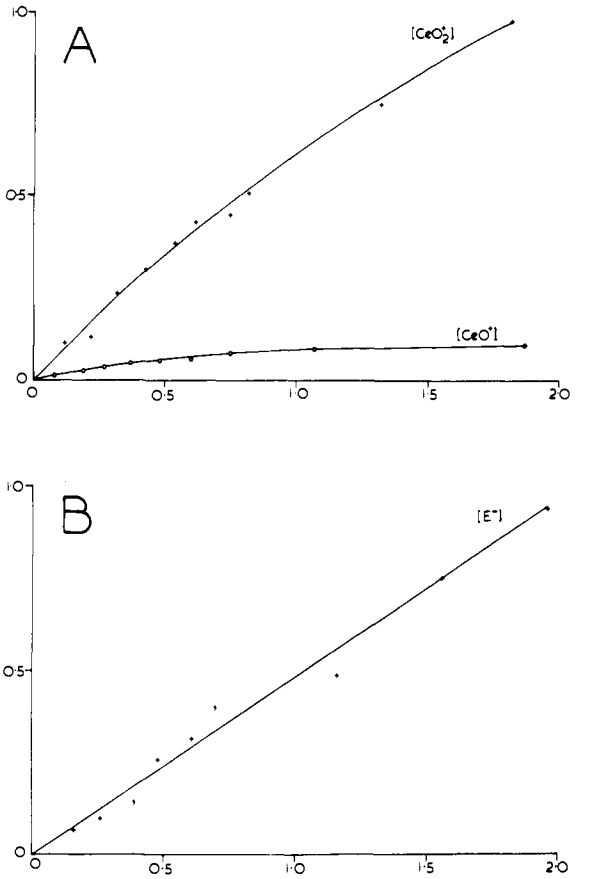

Figure 3. Experimental plots of [CeO_2^+], [CeO^+], and [e^-] as a function of total oxygen pressure: ordinate, relative intensity; abscissa, oxygen pressure from 0 to 2 × 10^{-3} Torr.

However, the most obvious reason for this difference is that secondary reactions are occurring under the effusive flow conditions used in the present work and these alter the CeO_2^+:CeO^+ ion intensity ratio from that observed under the molecular beam conditions of ref 12.

Possible reactions are

$$Ce + O_2 \rightarrow CeO + O \qquad \Delta H = -3.13 \pm 1.28 \text{ eV} \quad (5)$$

$$Ce + O \rightarrow CeO^+ + e^- \qquad \Delta H = -2.86 \pm 1.78 \text{ eV} \quad (6)$$

$$CeO^+ + O_2 \rightarrow CeO_2^+ + O \qquad \Delta H = +1.14 \pm 0.68 \text{ eV} \quad (7)$$

$$Ce + CeO_2^+ \rightarrow CeO^+ + CeO \qquad \Delta H = -6.17 \pm 1.94 \text{ eV} \quad (8)$$

Use of available thermodynamic data[16–18,24] allows the reaction enthalpies of these processes to be estimated as shown. To investigate the combined effects of reactions 1–8 under the conditions used, it was decided to measure the experimental [CeO_2^+] and [CeO^+] ion intensities and the chemielectron intensity as a function of oxygen reagent pressure and to model the combined effects of these reactions with use of rate constants evaluated from available cross sections. The method used in these kinetic modeling calculations is that of ref 25.

The experimental plots of CeO_2^+ and CeO^+ ion intensities as a function of total oxygen pressure are shown in Figure 3a. The CeO_2^+ ion intensity was found to exhibit an approximately linear dependence on oxygen pressure in the oxygen pressure range 1 × 10^{-5}–4 × 10^{-3} Torr, although at higher pressures the ion intensity leveled out and became effectively constant. Similar behavior was observed for CeO^+, with an approximately linear region followed by a plateau at higher pressures (see Figure 3A). However, for

(16) Kordis, J.; Gingerich, K. A. *J. Chem. Phys.* **1977**, *66*, 483.
(17) Ackerman, R. J.; Rauh, E. G.; Thorn, E. J. *J. Chem. Phys.* **1976**, *65*, 1027.
(18) Ackerman, R. J.; Rauh, E. G. *J. Chem. Thermodynam.* **1971**, *3*, 609.
(19) Huber, K. P.; Herzberg, G. *Molecular Spectra and Molecular Structure IV. Constants of Diatomic Molecules*; Van Nostrand Reinhold: New York, 1979.
(20) Hotop, H.; Bennett, R. A.; Lineberger, W. C. *J. Chem. Phys.* **1973**, *58*, 2373.
(21) Martin, W. C.; Zalubas, R.; Hagan, L. *Atomic Energy Levels—The Rare Earth Elements*; National Bureau of Standards: Washington, DC, 1978.
(22) Celotta, R. J.; Bennett, R. A.; Hall, J. L.; Siegel, M. W.; Levine, J. *Phys. Rev.* **1972**, *A6*, 631.
(23) Piacente, V.; Bardi, G.; Malaspina, L.; Desideri, A. *J. Chem. Phys.* **1973**, *59*, 31.
(24) Staley, H. G.; Norman, J. H. *Int. J. Mass Spectrom. Ion Phys.* **1969**, *2*, 35.
(25) Braun, W.; Herron, J. T.; Kahaner, D. K. *Int. J. Chem. Kinet.* **1988**, *20*, 51.

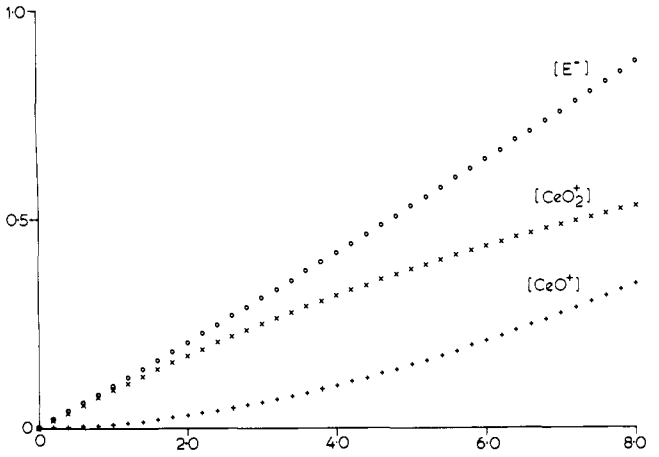

Figure 4. Calculated plots of $[CeO_2^+]$, $[CeO^+]$, and $[e^-]$ as a function of reaction time. See text for details of these calculations. Ordinate, relative intensity; abscissa, reaction time from 0 to 8.0 ms.

CeO^+ the onset of the plateau was observed at lower pressures than in the CeO_2^+ case. The total chemielectron intensity as a function of oxygen pressure is shown in Figure 3B. As in the CeO_2^+ case, approximately linear behavior was observed in the oxygen pressure range 1×10^{-5}–4×10^{-3} Torr. At slightly higher pressures the electron intensity leveled out and became approximately constant. Hence, as shown in Figure 3, the graph of electron intensity against oxygen pressure is very similar to that observed in the CeO_2^+ case but noticeably different from that observed for CeO^+.

To understand these results more fully, it was decided to carry out a computer simulation of the reaction scheme given by reactions 1–8. However, some problems were experienced because not all the cross sections (σ) for these reactions have been measured experimentally. Fite and co-workers[12] in their crossed-beam experiments have measured $\sigma_1 = 3 \times 10^{-19}$ cm^2, $\sigma_6 = 1 \times 10^{-16}$ cm^2, and $\sigma_2 + \sigma_3 = 1 \times 10^{-20}$ cm^2. To convert these cross sections into rate constants, use has been made of the standard formula[26]

$$k = \sigma\left(\frac{8k_BT}{\pi\mu}\right)^{1/2} = 1.46 \times 10^4\sigma\left(\frac{T}{\mu}\right)^{1/2} \text{ cm}^3 \text{ molecule}^{-1} \text{ s}^{-1}$$

Hence, for reactions 1 and 6, with a temperature of 1000 K, k_1 and k_6 are obtained as 2.7×10^{-14} and 1.3×10^{-11} cm^3 molecule^{-1} s^{-1}, respectively. Unfortunately, it is not possible to estimate k_2 and k_3 individually as only the combined cross section of reactions 2 and 3 has been measured. However, in studies of a large number of chemiionization reactions,[12] it has been consistently found that where a free-electron channel and a negative-ion channel compete (as in reactions 2 and 3), the free-electron channel always dominates. In fact, for the La + O_2 case the ratio of the cross sections $\sigma_3:\sigma_2$ has been measured as approximately 10:1.[12] With this in mind, σ_3 was taken as 0.9×10^{-20} cm^2 (and hence k_3 was evaluated as 1×10^{-15} cm^3 molecule^{-1} s^{-1}) and σ_2 was taken as 0.1×10^{-20} cm^2 (i.e., $k_2 = 1.2 \times 10^{-16}$ cm^3 molecule^{-1} s^{-1}). The problem now is to estimate rate constants for reactions 4, 5, 7, and 8. Reaction 8 is highly exothermic, and it seems reasonable to approximate k_8 to a value given by the collision frequency of 1×10^{-10} cm^3 molecule^{-1} s^{-1}, whereas reaction 4 is highly endothermic and is given a value of 10^{-18} cm^3 molecule^{-1} s^{-1}. Reaction 7 lies between reactions 1 and 3 in endothermicity, and therefore a value of $k_7 = 5 \times 10^{-15}$ cm^3 molecule^{-1} s^{-1} was thought reasonable. It only remains now to estimate a value for k_5. To do this, simulations were performed for k_5 values in the range 10^{-11}–10^{-14} cm^3 molecule^{-1} s^{-1} until the CeO_2^+:CeO^+ ratio approximately matched the experimental CeO_2^+:CeO^+ ratio at a reaction time of 4 ms, the reaction time after which the ion intensity ratio was measured experimentally, as estimated from flow-rate measurements. The initial concentrations of the reactants, cerium and oxygen, used in these calculations were each taken as 10^{12} molecules cm^{-3} as estimated from the reagent pressures used experimentally. The value of k_5 obtained by this route is 5×10^{-14} cm^3 molecule^{-1} s^{-1}. From these calculations, the CeO_2^+:CeO^+ ratio was computed as 3.1:1, a value that was thought acceptable in view of the approximate nature of the calculations. A plot of the computed $[CeO_2^+]$, $[CeO^+]$, and $[e^-]$ concentrations as a function of reaction time is shown in Figure 4. As can be seen, the CeO_2^+ concentration is greater than the CeO^+ concentration at reaction times up to 8 ms. Having obtained this plot, it is informative to look at the contributions from reactions 1–8 to the total CeO_2^+, CeO^+, and e^- concentrations in the reaction time range 0–10 ms. These plots are presented in Figure 5. Figure 5A shows that the main source of CeO_2^+ at these reaction times is reaction 1. Consistent with this, Figure 5C indicates that the main source of electrons is reaction 1, with very small contributions expected from reactions 3 and 6. In contrast, CeO^+ arises from a number of sources. Figure 5B shows that at a reaction time of 4 ms the largest source of CeO^+ is reaction 8 with appreciable contributions also arising from reactions 6 and 3.

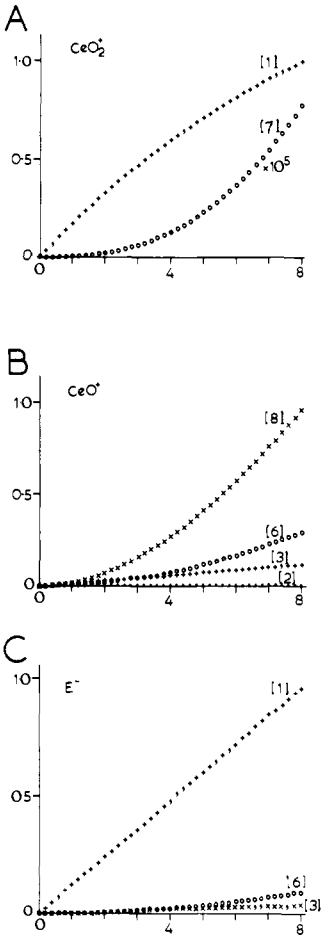

Figure 5. Calculated plots of $[CeO_2^+]$, $[CeO^+]$, and $[e^-]$ as a function of reaction time showing the relative contributions from reactions 1–8. See text for details of these calculations. (A) CeO_2^+, (B) CeO^+, (C) $[e^-]$. Ordinate, relative intensity; abscissa, reaction time from 0 to 8.0 ms.

Calculations were also performed to simulate the dependence of the $[CeO_2^+]$, $[CeO^+]$, and $[e^-]$ concentrations (at a reaction time of 4 ms) on the initial oxygen reagent pressure. The results of these calculations are shown in Figure 6. As can be seen, this figure shows the same general features as Figure 3, correctly reproducing the trend observed experimentally with the CeO^+ plot reaching a plateau at a lower total oxygen pressure than the CeO_2^+ and e^- plots.

Hence to summarize, although these simulations are highly approximate in that a number of the required rate constants are not available and "reasonable" values have had to be assumed,

(26) Fontijn, A. *Pure Appl. Chem.* **1974**, *39*, 287.

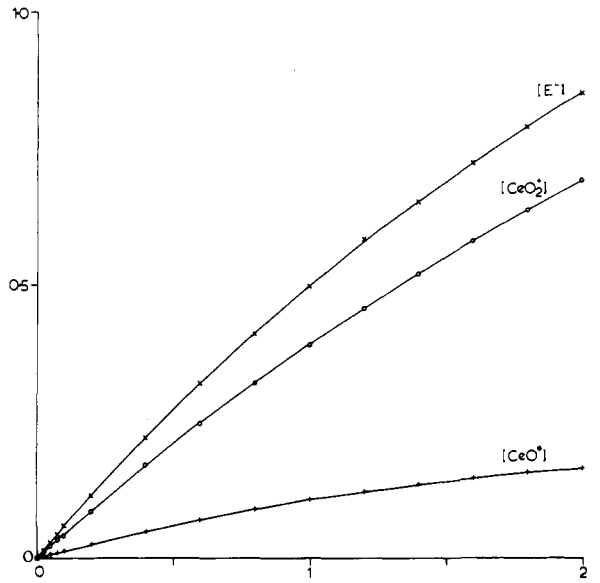

Figure 6. Calculated plots of $[CeO_2^+]$, $[CeO^+]$, and $[e^-]$ as a function of total oxygen pressure. See text for details of these calculations. Ordinate, relative intensity; abscissa, oxygen pressure from 0 to 2×10^{-3} Torr.

they do provide further support for the assignment of the chemielectron band in Figure 1 to the associative ionization reaction, reaction 1.

One other complication occurs in this work in that the electron energy analyzer used in these experiments is in principle unable to distinguish between electrons and negative ions that have the same kinetic energy. The question arises, therefore, as to whether O^- or O_2^- ions could contribute to the chemielectron band shown in Figure 1. Contributions from O_2^- can be ruled out immediately as these ions are produced only via reaction 4, which is very endothermic and expected to be very slow. In any case, no Ce^+ ions, the other product of reaction 4, could be detected experimentally. CeO^+ and O^- ions are produced by reaction 2, a reaction that is expected to have a low cross section relative to that of the competing process, reaction 3. Also, the most intense ion signal seen in this work from the Ce + O_2 reaction is CeO_2^+ with the CeO^+ intensity arising from reactions 3, 6, and 8. None of these reactions produce O^- ions and therefore it seems fairly certain that contributions of O^- to the chemielectron spectrum shown in Figure 1 can be ruled out. Apart from these considerations, it should be possible to apply a small magnetic field to distinguish between O^- ions and electrons. With this in mind, chemielectron spectra of the type shown in Figure 1 were recorded as a function of magnetic field, as applied by using the Helmholtz coils of the spectrometer. For fields of ±50 mG applied either parallel or perpendicular to the entrance slits of the spectrometer, the maximum of the chemiionization band was, within experimental error (±0.03 eV), unchanged with respect to the vibrational components of the fourth photoelectron band of oxygen recorded with HeI radiation. For a field of +50 mG applied parallel to the entrance slits, O^- ions with an energy of 1 eV are expected to remain unchanged in energy and undeflected by the field. The 1-eV electrons will also be unchanged in energy but will be deflected by the field. Approximate calculations show that these electrons will appear to double in energy when focused by the hemispherical analyzer on application of the above 50-mG field. Electrons associated with the fourth band of oxygen will also be deflected on application of this field and will appear to increase in energy when focused by the analyzer. As a result, if the band centered at 0.90 eV in Figure 1 arises from chemielectrons, both the chemielectron band and the fourth band of oxygen will move on application of a field, but the linearity of the energy scale will be retained, giving rise to no shift in the band at 0.90 eV electron kinetic energy. Alternatively, if the band at 0.90 eV in Figure 1 arises from O^- ions, this band would appear to move to lower energy, relative to the fourth band of oxygen, on application of

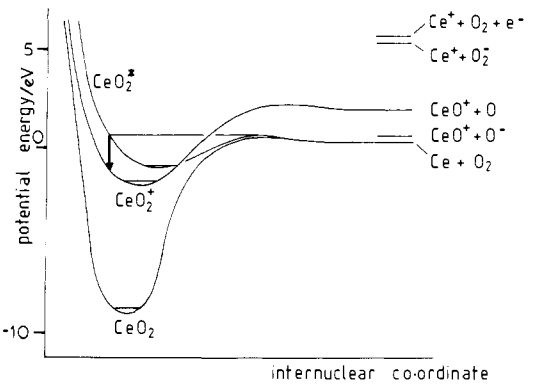

Figure 7. Schematic representation of the Ce + O_2 associative ionization reaction. The approximate energy scale of the vertical axis has been determined by using the results of this work and available thermodynamic data. The Ce + O_2 energy at infinite separation is, for convenience, taken as zero.

a magnetic field parallel to the slits. A field of +50 mG is expected to produce an *apparent* reduction in kinetic energy of the band in Figure 1 of ≈0.2 eV, whereas a field of −50 mG is expected to produce an apparent increase in the kinetic energy of the band in Figure 1 of ≈0.7 eV if it arises from O^- ions. However, no such change in position was observed, confirming assignment of the band centered at 0.9 eV in Figure 1 to electrons rather than O^- ions. All the evidence points therefore to the Ce + O_2 associative ionization reaction, reaction 1, being the dominant reaction in this investigation.

As mentioned earlier, vibrational structure with an average vibrational separation of 790 ± 30 cm^{-1} was observed in the chemielectron spectrum recorded for the Ce + O_2 reaction (see Figure 1). The only chemiionization mechanism that accounts for vibrational structure is the classical turning point mechanism,[6,27,28] and this is illustrated in Figure 7 where schematic potential energy surfaces for the reactants and products have been drawn. In this diagram, the reactants Ce + O_2 correlate with both the ground state of CeO_2 and an excited state, CeO_2*, which lies above the ground state of the ion, CeO_2^+, for a range of values of internuclear coordinates. As indicated in Figure 7, the reactants approach each other until at the left turning point of the CeO_2* surface autoionization takes place onto the CeO_2^+ surface. The observed vibrational structure corresponds to transitions to different vibrational levels of the CeO_2^+ state. Assignment of this structure to a particular vibrational mode in the ion is not straightforward, as the equilibrium geometries of CeO_2^+ and CeO_2* are not known. However, CeO_2 in its ground state is known to have a C_{2v} equilibrium geometry,[29-31] and the ν_1 and ν_3 modes for this state have been measured by recording the infrared spectra of this molecule isolated in an inert gas matrix as 757 and 737 cm^{-1}, respectively.[30,31] The bending mode, ν_2, was not observed in these spectroscopic studies but is expected to be below 200 cm^{-1}.[30,31] Hence, if the CeO_2^+ and CeO_2* states involved in the chemiionization process also have C_{2v} equilibrium geometries, the observed vibrational structure can be assigned to excitation of the ν_1 mode in the ion as the ν_3 mode would be forbidden in single quantum excitation.

Previous work by Young et al.[10] on the Ce + O_2 reaction, where relative cross sections of CeO_2^+, CeO^+, and Ce^+ production were measured as a function of relative collision energy between the reactants, indicated an apparent threshold for formation of CeO_2^+ of approximately 0.8 eV of relative collision energy. In contrast, no such threshold has been observed in the present work where

(27) Herman, Z.; Cermak, V. *Coll. Czech. Chem. Commun.* **1966**, *31*, 649.
(28) Nielson, S. E.; Berry, R. S. In *Recent Developments in Mass Spectrometry*; Ogatha, K.; Hayakowa, T.; Eds.; University Press: Baltimore, 1970.
(29) Kaufmann, M.; Muenter, J.; Klemperer, W. *J. Chem. Phys.* **1967**, *47*, 3365.
(30) DeKock, R. L.; Weltner, W. *J. Phys. Chem.* **1971**, *75*, 514.
(31) Gabelnick, S. D.; Reedy, G. T.; Chasanov, M. G. *J. Chem. Phys.* **1974**, *60*, 1167.

it has been shown that reaction 1 occurs at thermal collision energies. Currently available thermodynamic data are not of sufficient accuracy to indicate whether reaction 1 is endothermic or exothermic. However, it is clear from the results presented that this reaction must be exothermic to account for the observation of CeO_2^+ at thermal collision energies and the observation of chemielectrons with energies of ~ 1 eV. There is therefore clearly a need for more accurate thermodynamic data on the cerium–oxygen system. Nevertheless, the qualitative discussion presented in this paper demonstrates how chemielectron spectroscopy is capable of probing the potential energy surfaces of reacting systems and providing complementary information on molecular ions to that obtained from photoelectron spectroscopy. Related work is currently in progress on other lanthanide plus oxygen chemiionization reactions. In particular, the La + O_2, Pr + O_2, and Nd + O_2 reactions are being studied, and for these reactions available cross sections[12] suggest that the analogue of reaction 6 is faster than in the Ce + O_2 case.

Acknowledgment. We thank the SERC for financial assistance, and A.M.E. thanks the CEGB for the award of a CASE studentship. This work was also supported in part by the Air Force Office of Scientific Research (Grant No. AFOSR-89-0351) through the European Office of Aerospace Research (EOARD), United States Air Force.

Registry No. Ce, 7440-45-1; O_2, 7782-44-7.

Hydrogen-Abstraction Reactivity of Excited-State Para-Substituted Benzyl Radicals in Solution at Room Temperature

Kunihiro Tokumura,* Tomomi Ozaki, and Michiya Itoh

Contribution from the Faculty of Pharmaceutical Sciences and Division of Life Sciences, Graduate School, Kanazawa University, Takara-machi, Kanazawa 920, Japan.
Received August 12, 1988

Abstract: In contrast to almost no H-abstraction reactivity of the ground-state para-substituted benzyl radicals (*p*-X-benzyls: X = CN, Cl, F, and OCH_3) toward 1,4-cyclohexadiene (CHD), a significant fluorescence quenching by CHD in hexane at room temperature was confirmed for their fluorescent excited states, which may be assigned to $2B_2$ for *p*-cyanobenzyl and $1A_2$ for the other three *p*-X-benzyls. The quenching reveals a marked substituent effect: the quenching rate constant of 3.2×10^9 M^{-1} s^{-1} for *p*-cyanobenzyl fluorescence is much larger than that of 9.4×10^5 M^{-1} s^{-1} for *p*-methoxybenzyl fluorescence. The excited-state H-abstraction of *p*-cyanobenzyl from a H-donating CHD was directly demonstrated by the transient absorption induced upon the 308-nm pulse excitation of the ground-state *p*-cyanobenzyl. The marked substituent effect upon the quenching by CHD implies that $1A_2$ and $2B_2$ states have considerably different unpaired electron densities at the benzyl position.

Various multiphoton processes are operative in the organic photochemical reactions induced by intense laser pulses. One of the most efficient biphotonic processes is the photolysis of the transient species such as excited states and/or various reactive intermediates. Many free radicals are known as the reactive intermediate in the organic photochemistry. The study of the reactivity of the excited-state aromatic free radical would be thus expected to elucidate the laser-induced organic photochemistry, which is usually performed in the liquid phase at room temperature. Such a study (one of the photochemistry of transient species) is an attractive and current subject in the physical organic chemistry. The unimolecular rearrangement in the lowest excited doublet state has been confirmed for the very long-lived triphenylmethyl[1] and the stable perchlorotriphenylmethyl[2] radicals in solution at room temperature. Upon photoexcitation of unstable aromatic radicals (benzophenone ketyl[3] and the several arylmethyl radicals such as diphenylmethyl[4] and 1-naphthylmethyl[5]), furthermore, the intermolecular reactions with various substrates have been demonstrated to take place in solution at room temperature.[3-7] Long-lived excited-state radicals are generally preferable for the intermolecular reactions in fluid solution.

It has been demonstrated that the fluorescent-state benzyl radical (the prototype of arylmethyl radicals) in solution at room temperature is very short-lived (≤ 1 ns) owing to an extensively temperature-dependent nonradiative relaxation.[8,9] However, the fluorescence lifetimes of *p*-chlorobenzyl and *p*-methoxybenzyl in hexane at room temperature have recently been determined to be 81 ± 5[9] and 120 ± 5 ns,[10] which are much longer than that of benzyl. Such relatively long fluorescence lifetimes stimulated us to study the intermolecular reactivity of some para-substituted benzyls in the fluorescent excited state.

Based upon the kinetics and spectra of the fluorescence and absorption induced upon the 308-nm pulse excitation of the ground-state *p*-X-benzyl radical (X = OCH_3, F, Cl, or CN) in hexane at room temperature, we wish to report the quenching reaction of the excited-state *p*-X-benzyl by 1,4-cyclohexadiene known as a potential H donor. A pronounced substituent effect upon the quenching is discussed in terms of the $1A_2 \leftrightarrow 2B_2$ alternation of the lowest excited doublet state.

Experimental Section

p-(Chloromethyl)anisole (4-methoxybenzyl chloride, Tokyo Kasei), 4-fluorobenzyl bromide (Aldrich), and 4-chlorobenzyl chloride (Nakarai) were used after distillation under reduced pressure. α-Bromo-*p*-tolunitrile (4-cyanobenzyl bromide, Aldrich) was purified by recrystallization from

(1) Bromberg, A.; Schmidt, K. H.; Meisel, D. *J. Am. Chem. Soc.* **1985**, *107*, 83.
(2) Fox, M. A.; Gaillard, E.; Chen, C.-C. *J. Am. Chem. Soc.* **1987**, *109*, 7088.
(3) Nagarajan, V.; Fessenden, R. W. *Chem. Phys. Lett.* **1984**, *112*, 207.
(4) Scaiano, J. C.; Tanner, M.; Weir, D. *J. Am. Chem. Soc.* **1985**, *107*, 4396.
(5) Johnston, L. J.; Scaiano, J. C. *J. Am. Chem. Soc.* **1985**, *107*, 6368.
(6) Scaiano, J. C.; Johnston, L. J.; McGimpsey, W. G.; Weir, D. *Acc. Chem. Res.* **1988**, *21*, 22 and references therein.
(7) Johnston, L. J.; Lougnot, D. J.; Wintgens, V.; Scaiano, J. C. *J. Am. Chem. Soc.* **1988**, *110*, 518.
(8) Meisel, D.; Das, P. K.; Hug, G. L.; Bhattacharyya, K.; Fessenden, R. W. *J. Am. Chem. Soc.* **1986**, *108*, 4706.
(9) Tokumura, K.; Udagawa, M.; Ozaki, T.; Itoh, M. *Chem. Phys. Lett.* **1987**, *141*, 558.
(10) Tokumura, K.; Ozaki, T.; Udagawa, M.; Itoh, M. *J. Phys. Chem.* **1989**, *93*, 161.

0002-7863/89/1511-5999$01.50/0